An Energetic Based Method Leading to Merged Control Loops for the Stability of Input Filters

P. Barrade *, A. Bouscayrol **, P. Delarue**
* Laboratoire d'Electronique Industrielle
EPFL-STI-IEL-LEI
Station11
CH-1015 Lausanne, Switzerland
Philippe.barrade@epfl.ch

** L2EP
University of Lille 1
59 655 Villeneuve d'Asq cedex, France
alain.bouscayrol@univ-lille1.fr
philippe.delarue@univ-lille1.fr

***Abstract*- In most of applications, power converters are controlled to allow their output current/voltage to follow the required reference values. For DC/DC and DC/AC converters, the control must take into account their input voltage, which must be rejected. In such conditions, the converters can be modeled as negative impedance, causing the instability of their feeding 2nd order input filter. This paper presents an original method for the stabilization of the input filter. A merged control scheme is defined using an Energetic based method. A first control scheme is defined to control the output current. A second independent control scheme is defined to control the filter stability. Both control loops are merged using a weighing criterion. Simulation results are provided and the stability issue is discussed.**

I. INTRODUCTION

Converters fed by a DC voltage are often interfaced to their DC source by 2nd order low pass filters. Such filters are in most of the applications made of an LC cell. The aim is to feed the converter with a DC voltage where high frequency ripple is minimized. A second goal is to lower the harmonic content of the current absorbed on the DC supply.

In the case where the control of the converter is such as the average power it absorbs is constant, the input LC filter can become unstable. This instability is of course dependent of the parameters of the filter (the values of L and C). It is also dependent on resistive components linked to L and C. Moreover, the potential instability is dependent on the converter operating point (the average power it absorbs), and on the value of the DC feeding voltage.

Such a problem has been identified in the early 80's. Some deep studies have been performed by Cuk and Middlebrook [1][2]. They outline the input filter risk of instabilities. They propose models and design rules to solve such a problem. Their considerations and stability criteria are still today of a common use, and are the references in the field.

Since then, some complementary studies have been made, trying to improve the tools linked to the stability of input filters [3]. Moreover, if the initial researches were in the field of low- to mid-power applications, this topic is still under study in the frame of HVDC power distribution or weak DC microgrids, for mid- to high power applications [4][5], and for transportation systems.

The state-of-the-art today leads to solve the input filter stability problem thanks to two main solutions. The first one consists in adding to the LC input filter some damping cells (generally parallel RC branches). A resistive component is added to offer the global stability and the correct damping of the filter. The sizing process of the input filter is made with two main requests: filtering capabilities and stability. One must note in this case that this sizing process is decoupled from considerations on the control and on dynamic behavior of the converter fed by the input filter.

The second solution for the stabilization of the input filter consists is adapting the control of the converter, focusing not only on the regulation of its output voltage/current, but taking also into account the dynamic behavior of the input filter. There, the input filter is sized in terms of filtering capability and dynamic behavior, while the design of an appropriate control scheme for the power converter must take into account the dynamics of the input filter.

This last approach will be followed in this contribution, in the general frame of electric and hybrid vehicles. The aim is to identify the way the control scheme of a power converter can be designed to take into account the dynamic behavior of its input filter. An Energetic Macroscopic Representation (EMR) will be used [6]. This description enables the identification of control structures by a step-by-step inversion method. From the inversion-based control, the modeling of the structure and its control will demonstrate that the control structure stabilizes effectively the input filter. A new control scheme is proposed by merging two control loops.

II. INPUT FILTER INSTABILITIES

A. *Structure and conventional control scheme*

The origin of input filter instabilities is generally introduced by the step-by-step approach followed for the design of a system. Considering for example a battery charger for an electric vehicle, one design in a first step the converter needed to charge some batteries from a DC source as presented in Fig. 1.

The batteries are presented as a voltage source E_2, where a charging current I_s is injected from a bidirectional DC/DC converter *Cvs* via a current ripple limiter inductor L_s.

978-1-4244-8218-4/10/$26.00 ©2010 IEEE

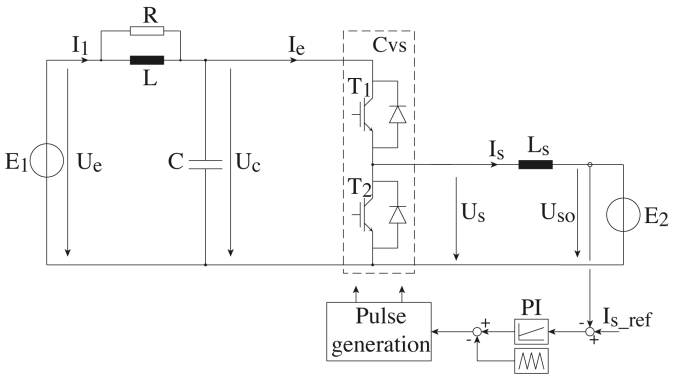

Fig. 1. Battery charger with an input filter – Generic control scheme for the output current regulation.

A *LC* filter is inserted between the primary voltage source E_1 to limit an eventual voltage ripple for feeding the converter. This input filter is also needed for limiting the harmonic content of the current from the main voltage source E_1. A resistor R is added to ensure the damping of the input filter.

In order to control the charging current I_s for the batteries, a control loop is needed, also presented in Fig. 1. As it is presented, this current control loop is in its simplest form. The error between a current reference I_{s_ref} and the measure of the current I_s is amplified with a PI controller. The result is injected in a PWM modulator that generates the control signals for triggering the two transistors T_1 and T_2.

Such a system behaves typically as it is presented in Fig. 2. Such a simulation result has been obtained with the following parameters: U_e=600, U_{so}=200V, L=L_s=10mH, C=0.3mF, R=36Ω. The switching frequency of the converter is f=10kHz. The proportional gain of the PI control is *50* while the integral gain is *10*.

As expected for such a simple system, the output current I_s follows its reference I_{s_ref} which is at first 20A, then 50A at 100ms and finally 45A at 400ms. However, the analysis of the input filter voltage U_c shows strong oscillations.

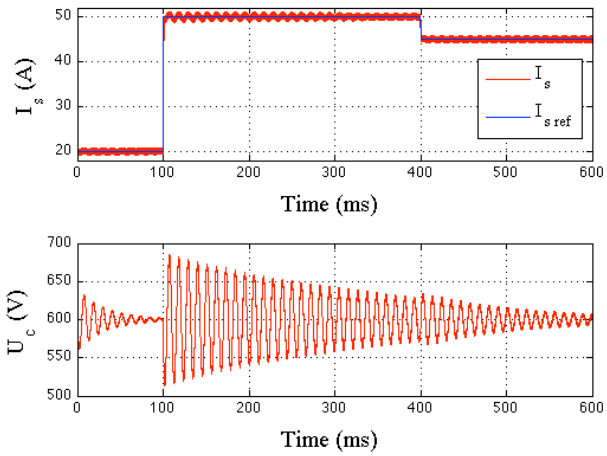

Fig. 2. Natural stability of the input filter when the current control loop does not reject the input filter voltage

They are due to the variations of the average value of the current I_e at each step on the output reference current.

One must note that these input filter oscillations impact on the output current I_s. It presents a non-negligible ripple at the oscillation frequency of the input filter. Moreover, the output current regulation has no possibility to reject the input filter oscillations, whatever is its structure and its sizing. This is in particular due to the identical values of L and L_s, as well as the low value of C. If the simple control scheme presented in Fig. 1 is maintained, the only possibility to lower the input filter oscillations is to act on the sizing of the damping resistor R, but it will impact the global efficiency of the system.

B. Rejection of the input filter oscillations

Independently of the necessity to damp the input filter oscillations, it is of a great interest to identify the possibility to cancel any low frequency ripple on the output current I_s due to the input filter oscillations.

For this, one can use the Energetic Macroscopic Representation methodology (EMR), applied to the structure defined in Fig. 1.

This EMR is presented in Fig. 3. It uses green and orange elements [6]. The green elements represent the electrical sources of the system (the DC bus E_1 and the batteries E_2). The orange elements represent respectively the converter (as a conversion element, with a transformation ratio defined by the duty cycle of the converter), the inductors L and L_s, as well as the capacitor C (as accumulation elements).

From this EMR, the second step consists in applying inversion rules following the objectives that have been assigned. It leads to a so-called inversion-based control [7]. The result appears also in Fig. 3 (blue elements). The control of the current has to be made thanks to a controller (PI kind), where the voltage E_2 on the batteries appears to be a perturbation that must be rejected. The result is the reference voltage U_{s_ref} needed at the output of the converter, easy to obtain by adjusting the duty cycle. For this, the input voltage U_c must be taken into account as a perturbation if not strictly constant. The dot line from U_c to the modulator that generates the duty cycles illustrates that the rejection of U_c is optional under particular conditions. It can be omitted when the input voltage of the converter varies slowly. This is not the case in the application we focus in this paper: the input filter voltage fluctuations are large, and their dynamic cannot be compensated directly with the output current regulator.

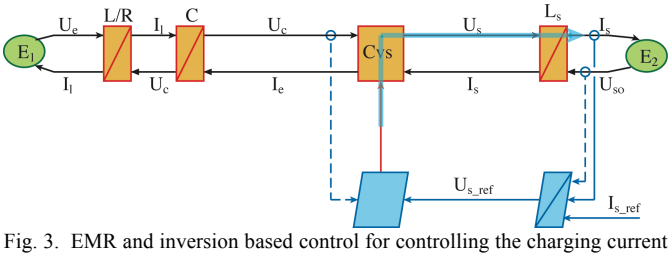

Fig. 3. EMR and inversion based control for controlling the charging current - Rejection of the voltage U_c

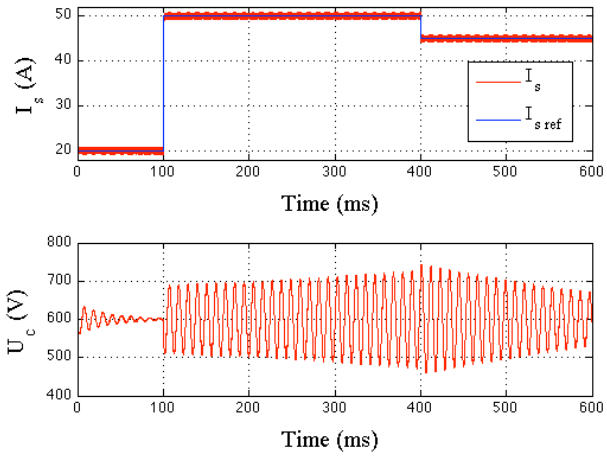

Fig. 4. Instability of the input filter when the current control loop reject the input filter voltage - The instability is a function of the operating point

When implemented, the reject of the input filter voltage by the output control loop leads to the instability of the input filter. It is illustrated in Fig. 4. One must note that this instability is dependent on the operating point: the input filter is stable when a *20A* or *45A* output current is requested. It is unstable when the output current is *50A*.

However, even if strong instabilities occur in the input filter, the output current regulation succeeds in maintaining the current I_s along its reference. A low frequency ripple can be observed, due to the input filter oscillations: the duty cycle of the converter is adjusted to compensate the variations of U_c. As a result, the output current ripple varies in magnitude with the variations of the duty cycle of the converter.

C. *Origin of the input filter instability*

The control scheme as defined in Fig. 3, used for the output current regulation of the converter presented in Fig. 1 is the origin of the input filter stability. As described above, the rejection of the voltage U_c enable the correct regulation of the output current. In other words, the output current I_s follows its reference whatever are the oscillations of the input filter.

In such conditions, the average input power absorbed by the converter *Cvs* is constant with no fluctuation at the resonant frequency of the input filter. Assuming, that this constant power is P_o, one can then define:

$$P_o = U_c I_e \tag{1}$$

The derivative of (1) gives:

$$0 = I_e \delta U_c + U_c \delta I_e \Rightarrow Z_d = \frac{\delta U_c}{\delta I_e} = -\frac{U_c}{I_e} \tag{2}$$

Z_d is the converter input impedance. It is a negative impedance, which loads the input filter. Without any resistance, the input filter is unstable in any case. From (1) and (2), one can also establish:

$$Z_d = -\frac{{U_c}^2}{P_o} \tag{3}$$

Equation (3) shows that the absolute value of the converter input impedance depends on the operating point with P_o. For a given damping resistor R, the input filter can be stable or unstable depending on P_o. This is the reason why the simulation results in Fig. 4 show the stability of the input filter for a *20A* or *45A* output current. Anyway, the input filter is unstable for a *50A* output current.

Even in the cases where the input filter is stable (I_s<*50A*), its damping is also a function of the operating point.

III. Merged Control for Input Filter Stabilization

A. *General considerations*

The aim of the following developments is to allow the respect of the current regulation as described in Fig. 3, while the stabilization of the input filter is enabled. By stabilization of the input filter, we mean the stability of the filter along all the operating points that can be reached by the system in Fig. 1, with a significant damping.

The most common solution is generally to size the input filter and its damping resistance is order to match these requirements. But this cannot be made without impairing on the global efficiency of the conversion.

Another possibility is to act on the control level of the converter. There, the filter is sized in filtering criteria only, while the control of the converter must acts following two objectives. The first one is the correct regulation of the converter output current. The second objective is the stabilization and the damping of the input filter.

One must remain that the main goal of the application defined in Fig. 1 is to control the charging current in batteries. This is the reason why the two objectives we have mentioned above must be classified. The first objective (output current regulation) is considered as the main objective. The second objective (input filter stability) is an additional objective. Its impair on the main objective must be lowered.

B. *Objectives and tuning parameter*

Regarding the two objectives we have defined for the control of the convert, one can analyze again the EMR related to the system in Fig. 1. This EMR is presented in Fig. 5.

From the two objectives we have defined, one must identify the control chains. These chains link the state variables associated with the objectives to the tuning parameters of the system. The tuning parameters are the parameters that allow the control of the system (the duty cycle of a converter for example).

For the first objective, the state variable to control is the output current I_s.

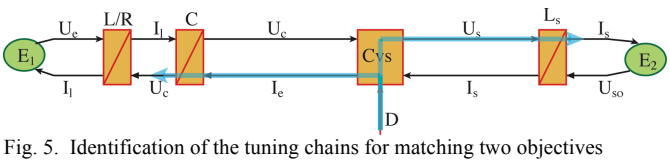

Fig. 5. Identification of the tuning chains for matching two objectives

Following inversion rules, I_s can be controlled with the appropriate control of the output voltage of the converter U_s, fixed by the duty cycle D of the converter. A first tuning chain linked to the first objective is then identified, from D to I_s.

For the second objective (stability of the input filter), one can decide to control the voltage U_c across the capacitor C. Still following inversion rules, U_c can be controlled with the appropriate control of the input current of the converter I_e, fixed by the duty cycle D of the converter. A second tuning chain is also identified, from D to U_c.

The two tuning chains we have identified as an answer to the two objectives appear both in Fig. 5 (large blue arrows). Their representation on the EMR shows that even if it is possible to identify two distinct tuning chains as an answer to the two initial objectives, there is only one single tuning parameter: the duty cycle D.

One has then to fulfill two constraints, for only one tuning parameter. This is this difficulty we intend to solve on the following approach.

C. *Merged control loops*

From the EMR in Fig. 5, one can consider separately the two constraints to obtain the inversion-based control for each of the two tuning chains. This is illustrated in Fig. 6.

At first, the tuning parameter (the duty cycle D of the converter) is affected to the control of the output current. It leads to the implementation of an output current regulation that generates a first reference duty cycle D_i for controlling the power converter.

If the control design is stopped there, then the results are strictly equivalent to what was done in Fig. 3 because $D=D_i$. Only the output current I_s is regulated, with the rejection of the filter voltage U_c and the risks of unstability of the input filter.

In a second step, the tuning parameter (the duty cycle D of the converter) is affected to the control of the voltage on the filter capacitor C. This is done without considering the previous step. It leads to the implementation of a capacitor voltage regulation that generates a second reference duty cycle D_u for controlling the power converter.

The two control loops that have been identified are presented in Fig. 6 (blue elements). They are directly obtained by conventional inversion rules following the two control chains that we have defined.

As we have defined two independent control loops, the result is then the generation of two duty cycles, D_u and D_I. Each of these duty cycles is affected to one objective: the correct regulation of the output current I_s for D_i, and the stability of the input filter for D_u. And even if two duty cycles are defined, there is only one for controlling the converter.

This last difficulty can be solved considering that once the two control loops are defined, the static converter *Cvs* can be considered as a coupling bloc in an EMR representation. The inversion of such a coupling element leads to distribution element in the inversion-based control (blue element made of two inserted rectangles).

The distribution element generates the duty cycle D needed for controlling the converter. This is done by an arbitrary combination of the two duty cycles D_u and D_i considered as inputs for the distribution element.

The combination of D_u and D_i is operated along the weighting factor k_w. If the identification of the two control loops and their merging via a distribution element result of a methodological approach, the generation of D from the two duty cycles D_u and D_i is arbitrary.

For this contribution, considering that the weighting factor k_w can be adjusted from *0* to *1*, one have chosen the following combination:

$$D = k_w D_u + (1 - k_w) D_i \tag{4}$$

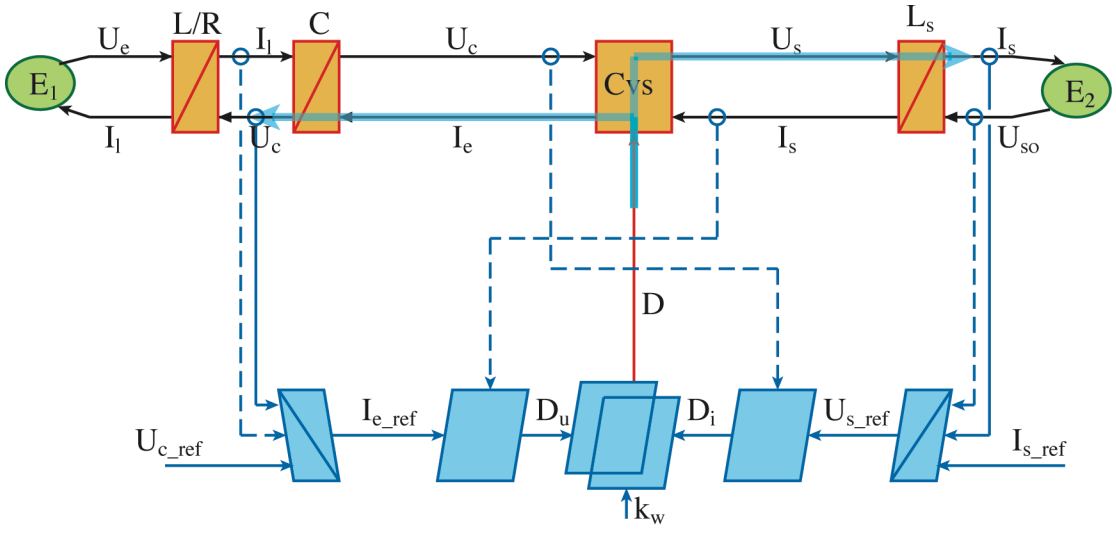

Fig. 6. Parallel control loops

IV. Analysis of the Merged Control Performances

A. System modeling

We have deduced a control structure presented in Fig. 6. One must then model the system and its control in order to validate that such a control scheme allows the stabilization of the input filter.

From Fig. 1, one can deduce the open loop average model of the considered system. It leads to a set of 3 equations linked to the 3 state variables of the systems:

$$\begin{aligned} C\dot{U}_c &= \frac{1}{R}(U_e - U_c) + I_l - DI_s \\ L\dot{I}_l &= U_e - U_c \\ L_s\dot{I}_s &= DU_c - U_{so} \end{aligned} \tag{5}$$

Regarding the definition of the duty cycle D in (4), one can explicit its definition by the definition of the two duty cycles D_u and D_i:

$$\begin{aligned} D_u = \frac{I_{e\_ref}}{I_s} &= \frac{1}{I_s}\left(-k_p(U_e - U_c) + I_l + \frac{1}{R}(U_e - U_c)\right) \\ D_i &= \frac{U_{s\_ref}}{U_c} \end{aligned} \tag{6}$$

The duty cycle D_i is defined as it appears in the inversion-based control in Fig. 6. The duty cycle D_u is defined the same way, by the ratio of I_{e_ref} and I_s. I_{e_ref} has been replaced by its definition: it comes from the regulation of U_c with a simple proportional controller (gain k_p), with the rejection of I_l and the rejection of the current into the damping resistor R. The reference voltage is $U_{c\_ref}=U_c$.

The definitions of the two duty cycles D_u and D_i are merged thanks to (4). The resulting definition of the duty cycle D is injected in (5). The system with the closed loop for the filter stabilization is finally modeled according the following equation:

$$\begin{bmatrix} \dot{U}_c \\ \dot{I}_l \\ \dot{I}_s \end{bmatrix} = A\begin{bmatrix} U_c \\ I_l \\ I_s \end{bmatrix} + B\begin{bmatrix} U_e \\ U_{s\_ref} \end{bmatrix} \tag{7}$$

One must precise that this last step leads to a non-linear system of differential equations. In order to solve it, a linearization has been made along a given operating point (small signal hypothesis). The matrix A is given in (8):

$$A = \begin{bmatrix} \frac{k_w - 1}{RC} - \frac{k_w k_p}{C} + \frac{P_o(1-k_w)}{CU_e{}^2} & \frac{1-k_w}{C} & \frac{-U_{so}(1-k_w)}{CU_e} \\ -\frac{1}{L} & 0 & 0 \\ \frac{k_w}{L_s}\left(\frac{U_{so}}{U_e} + \frac{U_e}{I_{so}}\left(k_p - \frac{1}{R}\right)\right) & \frac{U_e k_w}{L_s I_{so}} & \frac{-U_{so}k_w}{L_s I_{so}} \end{bmatrix} \tag{8}$$

The matrix B is defined in (9):

$$B = \begin{bmatrix} \frac{1}{C}\left(\frac{1}{R} - \frac{k_w}{R} + k_w k_p\right) & -\frac{I_{so}(1-k_w)}{CU_e} \\ \frac{1}{L} & 0 \\ \frac{k_w U_e}{L_s I_{so}}\left(\frac{1}{R} - k_p\right) - \frac{U_{so}}{L_s U_e} & \frac{1-k_w}{L_s} \end{bmatrix} \tag{9}$$

The operating point is defined with the two voltages U_e and U_{so}. It is also defined by the requested output current I_{s_ref}. In order to simplify the expressions of the matrix A and B, one has defined $I_{s\_ref}=I_{so}$ and $P_o = U_{so}\, I_{so}$.

Equation (7) is then used to identify the transfer functions defined in (10), where is also expressed the definition of the reference voltage U_{s_ref}, obtained for the control of the output current I_s thanks to a PI controller $C(s)$. The output voltage U_{so} is rejected as a perturbation according to the inversion-based control in Fig. 6:

$$\begin{aligned} F_{Uc}(s) &= \frac{U_c(s)}{U_{s\_ref}(s)} \\ F_{Is}(s) &= \frac{I_s(s)}{U_{s\_ref}(s)} \\ U_{s\_ref}(s) &= C(s)\left(\underbrace{I_{s\_ref}}_{I_{so}} - I_s\right) + U_{so} \end{aligned} \tag{10}$$

This last set of equations enable the identification of the closed loop transfer function of the system. As we focus on the stability of the input filter, the transfer function we will consider is the transfer function defined as $F_s(s)=U_c(s)/I_{so}(s)$.

B. Stability analysis

We will focus our analysis on the denominator $D(s)$ of the transfer function $F_s(s)$ as the poles of this function define the dynamic behavior of the system. $D(s)$ is defined by the equation:

$$D(s) = a_0 s^4 + a_1 s^3 + a_2 s^2 + a_3 s + a_4 \tag{10}$$

The coefficients a_0, a_1, a_2, a_3 and a_4 are functions of R, L, L_s and C. They are functions of the gains for the output current controller, as well as function of the two gains k_p and k_w for the input filter stabilization.

They are also functions of the operating point defined by U_e, U_{so} and $I_{s\_ref}=I_{so}$. As already mentioned, it means that the dynamic behavior of the input filter depends on the operating point. The expressions for a_0, a_1, a_2, a_3 and a_4 are not given in this article, as they are too complex. Dominant poles are thus defined, and an equivalent second order system can be defined with an oscillation frequency (ω_n) and a damping factor (ξ).

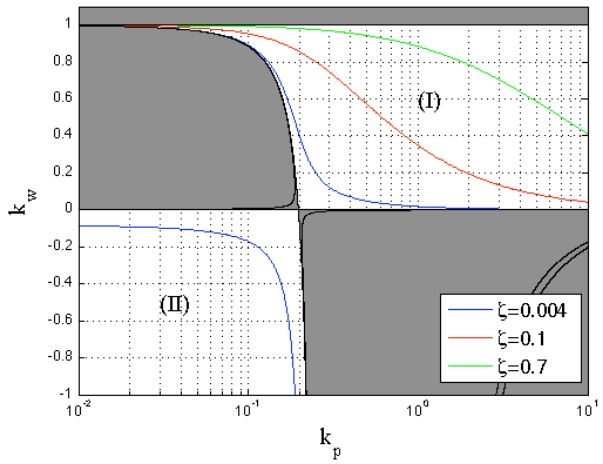

Fig. 7 Stability and dynamic properties analysis as functions of the input filter stabilization loop

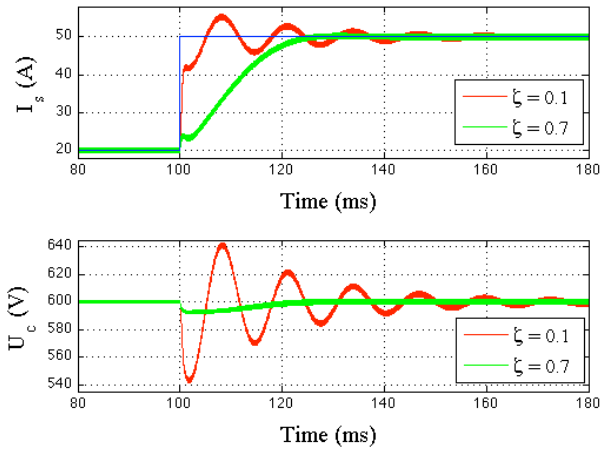

Fig. 8 Input filter stability

One consider the same parameters than those defined in section I, and for $I_{s\_ref}=I_{so}=50A$ where the input filter is unstable (Fig. 4). One has analyzed the impact on the stability of adding a control loop for the input filter stabilization by varying the parameters k_p and k_w. This has been made thanks to the calculation of the roots of $D(s)$. The results are given in Fig. 7.

The gray zones define values of k_p and k_w where at least one pole has a positive real value. The system is there unstable. It is in particular unstable for $k_w=0$. In this case, the loop for the input filter stabilization is not active, and it is a confirmation of the comments made in section I related to the instabilities of input filters.

The system is also unstable for $k_w=1$. In this case, the loop for the output current is not active. Even if the input filter can be stabilized, the duty cycle generated for this does not necessarily match the duty cycle required for the control of the output current, that can diverge.

The zone of the plan (k_p,k_w) where the stability can be obtained are noted (I) and (II) in Fig. 7. The zone (II) is not interesting, even if it defines the stability of the system. Indeed, the damping of the system is low despite large values of k_p and k_w. Moreover, negative values of k_w can lead to potential large values for the global duty cycle D. This can cause a lost of the system control due to the limitation of D between 0 and 1.

The only zone of interest is the zone (I), where the stability can be obtained, with a large set of possible choices for (k_p,k_w) to fix the damping ξ of the system to a required value.

This is illustrated in Fig. 8, where simulations have been made from the simulation initially proposed in Fig. 4. Here, the control loop for the input filter stabilization is implemented according the control structure proposed in Fig. 6. One have focus on the output current reference step from 20A to 50A that was initially unstable. From the abacus Fig. 7, one has chosen $k_p=1$. For a damping factor $\xi=0.1$, $k_w=0.36$, while $k_w=0.89$ for $\xi=0.7$.

The input filter behaves then as expected: it is stable, and its damping factor can be adjusted thanks to k_p and k_w.

One must note that for a damping factor $\xi=0.7$, the stability is obtained thanks to the lowering of the dynamic of the output current control in case of current reference step. There, the dynamic is mainly defined by the input filter dynamic.

V. Conclusion

This paper has presented an original method for the stabilization of DC/DC input filters. It led to merge two control loops, using only one single tuning parameter to match to control objectives.

The modeling of the closed loop system has shown that the control structure we have proposed allows effectively the correct output current control together with the input filter stabilization. It allows also the tuning of a required dynamic behavior

References

[1] R.D. Middlebrook, S. Cuk, “A general unified approach to modelling switching converters power stages”, IEEE PESC Rec. pp 18-34, 1976.

[2] R.D. Middlebrook, “Input filter considerations in design and application of switching regulators”, IEEE Industry Applications annual meeting, 1976

[3] P. Barrade, “Comportement dynamique des ensembles filter-convertisseur”, PhD thesism Institut National Polytechnique de Toulouse, France, 1997.

[4] F. Barruel, N. Retiere, J. Schanen, A Caisley, “Stability approach for vehicles DC power network: application to aircraft on-board system”, Power Electronics Specialists Conference, PESC’05, pp 1163-1169, june 16th, 2005.

[5] X.G. Feng, J.J. Liu, F.C. Lee, “Impedance specifications for stable DC distributed power systems”, IEEE Transactions on Power Electronics, vol. 17, pp. 157-162, 2002.

[6] Ph. Delarue, A. Bouscayrol, A. Tounzi, X. Guillaud, G. Lancigu, “Modelling, control and simulation of an overall wind energy conversion system", Renewable Energy, vol. 28, no. 8, pp. 1159-1324, July 2003.

[7] K. Chen, A. Bouscayrol, W. Lhomme, "Energetic macroscopic representation and inversion-based control: application to an electric vehicle with an electrical differential", Journal of Asian Electric Vehicles, Vol. 6, N°. 1, pages. 1097-1102, 6-2008.